






Article

Novel Copper Oxide Phyto-Nanocatalyst Utilized for the Synthesis of Sustainable Biodiesel from *Citrullus colocynthis* Seed Oil

Aqsa Aziz ¹, Mushtaq Ahmad ^{1,2}, Muhammad Zafar ^{1,*} , Abdel-Rhman Z. Gaafar ³ , Mohamed S. Hodhod ⁴, Shazia Sultana ¹, Mohammad Athar ⁵, Fethi Ahmet Ozdemir ⁶, Trobjon Makhkamov ⁷ , Akramjon Yuldashev ⁸ , Oybek Mamarakhimov ⁹, Maxsuda Nizomova ¹⁰, Salman Majeed ^{1,11}  and Bisha Chaudhay ¹

- ¹ Plant Systematics and Biodiversity Lab Department of Plant Sciences, Quaid-i-Azam University, Islamabad 45320, Pakistan; mushtaqflora@hotmail.com (M.A.); salmansunny61@gmail.com (S.M.)
- ² Pakistan Academy of Sciences, Islamabad 44000, Pakistan
- ³ Department of Botany and Microbiology, College of Science, King Saud University, Riyadh P.O. Box 11451, Saudi Arabia; agaafar@ksu.edu.sa
- ⁴ Faculty of Biotechnology, October University for Modern Sciences & Arts, 6th October City 12566, Egypt; mshodhod@msa.edu.eg
- ⁵ California Department of Food and Agriculture, Pest Detection & Emergency Projects, 1220 'N' Street, 2nd Floor, Sacramento, CA 95814, USA
- ⁶ Department of Molecular Biology and Genetics, Faculty of Science and Arts, Bingol University, Bingol 12000, Turkey
- ⁷ Department of Forestry and Landscape Design, Tashkent State Agrarian University, 2 A., Universitet Str., Kibray District, Tashkent 100700, Uzbekistan
- ⁸ Department of Ecology and Botany, Andijan State University, 129, Universitet Str., Andijan 170100, Uzbekistan
- ⁹ Department of Ecology Monitoring, National University of Uzbekistan, 4 University Street, Tashkent 100174, Uzbekistan
- ¹⁰ Department of Medicinal Plants, Tashkent State Agrarian University, 2 A., Universitet Str., Kibray District, Tashkent 100700, Uzbekistan
- ¹¹ Department of Botany, University of Mianwali, Mianwali 42200, Pakistan
- * Correspondence: zafar@qau.edu.pk



Citation: Aziz, A.; Ahmad, M.; Zafar, M.; Gaafar, A.-R.Z.; Hodhod, M.S.; Sultana, S.; Athar, M.; Ozdemir, F.A.; Makhkamov, T.; Yuldashev, A.; et al. Novel Copper Oxide Phyto-Nanocatalyst Utilized for the Synthesis of Sustainable Biodiesel from *Citrullus colocynthis* Seed Oil. *Processes* **2023**, *11*, 1857. <https://doi.org/10.3390/pr11061857>

Academic Editors: Chiing-Chang Chen and Yu-Cai He

Received: 1 May 2023
Revised: 4 June 2023
Accepted: 15 June 2023
Published: 20 June 2023



Copyright: © 2023 by the authors. Licensee MDPI, Basel, Switzerland. This article is an open access article distributed under the terms and conditions of the Creative Commons Attribution (CC BY) license (<https://creativecommons.org/licenses/by/4.0/>).

Abstract: The green chemistry method for nanocatalyst synthesis along with environmentally feasible non-edible sources are promising alternatives to fossil fuels. The current study focuses on the synthesis of copper oxide phyto-nanocatalyst and the identification of a new renewable feedstock, *Citrullus colocynthis*, to reduce environmental pollution. The highest biodiesel yield (95%) was obtained under optimum conditions of a 1:8 oil-to-methanol ratio and reaction temperature of 85 °C for 120 min with a 0.365 wt% catalyst concentration. The phyto-nanocatalyst was synthesized using seed oil cake after extracting oil with the salt of copper (copper oxide). The catalyst was then subjected to various analyses, namely, EDX, FT-IR, SEM, and XRD. The catalyst was proved to be efficient and effective after being reused five times and still there was a very small difference in biodiesel yield. All the analyses also show sustainable and stable results. Thus, copper oxide phyto-nanocatalyst with non-edible *Citrullus colocynthis* proved to be highly effective, sustainable, and a better alternative source to the future biodiesel industry.

Keywords: biocatalyst; colocynth; green fuel; non-edible feedstock; renewable energy

1. Introduction

The continuous increase in world population results in higher demand for services and goods which eventually leads to greater energy consumption. Energy is a key factor in developing a global economy [1]. About 90% of industrially manufactured energy is driven by fossil fuels (crude oil, coal, and gas), which are a type of non-renewable energy [2]. The price fluctuation and environmental concerns regarding CO₂ gas emission from fossil

fuels [3], such as smog, global warming, and decreased biodiversity [4,5], led to the search for a reliable alternative energy. One of the potential alternative sources of sustainable energy source is biodiesel, which has a lower amount of greenhouse gas (GHG) emission [6].

Globally, almost 95% of commercial biodiesel is produced from edible oils [7]. Several countries around the world are exploiting their native resources for the production of biodiesel. A variety of feedstocks can be utilized for the production of biodiesel, comprising various types of vegetable oils, microbial oils, animal fats, and waste oils [8]. However, the utilization of edible oil for the production of biodiesel eventually resulted in a food versus fuel debate. This problem has raised the biodiesel cost to twice the price of petrodiesel [9].

However, non-edible oils are a favorable and good choice for the production of biodiesel. The proximity of non-edible seed oils is linked to the geography, climate of the region, indigenous flora, and soil [10]. Using non-edible oil for the synthesis of biodiesel has many advantages such as reducing the price of raw materials and also preventing competition in food [11]. Indigenous non-edible feedstock biodiesel synthesis may significantly reduce the overall cost of the process and air pollutants. If non-edible seed oil crops are grown on unfruitful soil, biodiesel can be a helpful energy crisis solution [12]. Non-edible oil feedstocks have been produced worldwide at an affordable price and high return regardless of land conditions and weather. Many researchers have recently reported the use of non-edible oil-yielding biodiesel seeds. *Jatropha*, *kapok*, *pongamia* [13], rubber seed, and rubber beaver oil are non-edible oil-production sources [14], which provide increased potential for biodiesel synthesis over edible oils. Non-specific environmental conditions are not necessary for non-edible oil-producing plants, as these species are perfectly adapted to growing in salt, infertile, and sodium-rich soils [15].

The biodiesel synthesis using different techniques is practically employed. Viscosity is the main problem that prevents vegetable oils from being used in diesel engines [16]. Other problems such as low cetane number and high flash point of the oils could also lead to low combustion and knocking. Such problems can be solved by applying different methods, such as pyrolysis, dilution/blending, micro-emulsion, and transesterification [17].

The most convenient method used for biodiesel production from oil and fat feedstocks is transesterification. Through transesterification, vegetable oils and fats (triglycerides) are transformed into their alkyl esters with decreased viscosity, almost the same as petro fuel [18]. In this reaction, one mole of fatty acid reacts with three moles of alcohol [19]. In general, transesterification is a kind of reversible reaction, which significantly proceeds in a forward direction under heat or pressure, although the rate of the reaction can be accelerated with the addition of a catalyst. Numerous researchers have reported varying molar ratios of oil to alcohol in order to obtain the optimal concentration of fatty acid methyl esters. To obtain 98% biodiesel, a 1:4 molar ratio of oil to alcohol is used at a temperature of 350–400 °C [20]. The molar ratio of oil to alcohol has an effect on the cost of untreated methanol evaporation. The primary factors that affect the rate of transesterification are the amount and type of catalyst used, the type of alcohol used, the reaction time and temperature, the free fatty acid content of the oils, and the water content of the oils [21].

The transesterification reaction can be classified into two types, i.e., non-catalytic and catalytic method. The catalytic transesterification can be catalyzed by heterogeneous or homogenous catalysts (acid or base). For the present research study, transesterification reaction is employed by including the catalytic or non-catalytic method [22]. Biodiesel synthesis is based on the catalysts' viability, efficient recovery, and product yield [23].

The most widely employed method for biodiesel production is homogenous alkali-catalyzed transesterification reaction [24]. The base catalysts are extremely active and cost effective, resulting in high-quality biodiesel in a short period of time [25]. The most widely used alkali catalysts in transesterification reaction are KOH and NaOH. A homogenous base catalyst has many significant advantages compared to an acid catalyst such as: (a) short time interval for increased biodiesel yield, (b) easy accessibility at lower cost, and (c) mild favorable reaction conditions. Reference [26] reported that alkali-based homogenous transesterification accelerates the reaction 4000 times faster than an acid cata-

lyst [27]. However, alkali-catalyzed transesterification has some drawbacks, one of which being that it is extremely sensitive to the FFA content of vegetable oils and fats. A high FFA content (>11) eventually results in the formation of soap, which reduces the efficiency of the catalyst, increases viscosity and gel formation, and complicates the glycerol separation process [28]. Heterogeneous catalysts are solid in nature and have a major advantage of easy recovery and separation from the reaction medium and reusability of the used catalyst. Hence, heterogeneous catalysis is thought to be a green method [29]. Numerous solid base catalysts, such as alkali earth metal oxides, hydrotalcites, and essential zeolites, are synthesized for biodiesel production [30]. Heterogeneous catalysts offer many benefits over homogenous catalysts: (a) longer lifespan and recyclable nature, (b) no soap formation and easy separation of product, (c) no need of washing the product and hence no water pollution, and (d) environmentally friendly and non-corrosive [31]. Among heterogeneous catalysts, calcium oxide was preferred due to its good performance, ready availability and low cost, and mild reaction conditions [32]. The primary issue with heterogeneous catalysts is the deactivation of the catalyst after multiple applications, resulting in leaching, coking, and poisoning [33].

Biodiesel synthesis using nanocatalysts has high potential over conventional alkali/acid catalysts in terms of their benefits. Nanocatalysis implies the utilization of several nanomaterials as a catalyst in different heterogeneous catalytic processes. Nanocatalysts have high catalytic efficiency, high surface-to-volume area, and high surface energy. In general, nanocatalysts enhance the reaction process, by permitting a low temperature requirement, energy consumption recovery, high recycling rates, and reducing the side reactions [34,35]. Nanocatalysts are of considerable interest due to their large surface area, which results in variations in their physical and chemical properties (e.g., catalytic activity, melting point and optical absorption, biological and satirical properties, electrical and temperature conductivity, and mechanical properties), in comparison to most of the same chemical properties [36].

Green synthesis is an environmentally safe approach that provides a unique practical chemistry tools to eliminate toxic waste, reduce energy intake, and use ecological solvents (water, ethanol, ethyl acetate, etc.). It is an environmentally friendly approach for the synthesis of nanocatalysts that applies to large-scale production. The plant-produced nanocatalyst is more efficient, stable, and faster to operate. The nanocatalysts display completely improved and new properties based on specific features such as morphology, size, and distribution [37]. There are many methods available to produce nanocatalysts, i.e., physical, electrochemical, photochemical, irradiative, and biological methods [38]. There are several drawbacks linked with chemical and physical methods of nanocatalyst synthesis such as usage of high pressure and temperature, toxic chemicals, and production of harmful by-products. Hence, it is essential to find an alternative method to produce nanocatalysts. Biological synthesis of nanocatalysts using extracts have been recommended as a chief substitute to conventional chemical plant methods as it reduces the use of high temperatures and toxic chemicals [39].

Pakistan has distinct flora. Pakistan's future for sustainable energy has immense potential and fortune. Taking all these favorable factors into account, some potential non-edible feedstocks throughout the country have been selected for the current research work. No systemic studies on such potential non-edible *Citrullus colocynthis* feedstock have been conducted according to the literature review. However, no data on the oil profile, application, and optimization of biodiesel are available as a potential source for biodiesel production. This study constitutes the first complete and comprehensive report on morphology of non-edible oil seed, oil characterization (quantitative and qualitative), phyto-nanocatalyst synthesis, and biodiesel synthesis via ASTM methods of transesterification, characterization, and standardization.

2. Materials and Methods

2.1. Compounds and Reagents

The chemicals and reagents employed in the present research work are copper sulfate pent hydrate ($\text{CuSO}_4 \cdot 5\text{H}_2\text{O}$), aluminum nitrate, sodium hydroxide (NaOH), sulfuric acid (H_2SO_4), isopropyl alcohol, ethanol, acetone, anhydrous methanol (CH_3OH), phenolphthalein, and chloroform (CHCl_3). All chemicals were of analytical grade and were obtained from Sigma Aldrich (USA) and Merck (Germany). n-Hexane, methanol (CH_3OH), potassium hydroxide (KOH), copper sulfate (CuSO_4), sodium hydroxide (NaOH), anhydrous sodium sulfate (Na_2SO_4), aluminum sulfate (Al_2SO_4), isopropanol, and phenolphthalein are all chemicals.

2.2. Collection of Non-Edible Oil Seeds

For seed collection, extensive field trips and surveys were conducted all over Pakistan. The seeds of *C. colocynthis* were collected by making consistent field visits around Mandi Yazman district Bahawalpur. The fruit's hard covering was manually separated from the seeds. Then, seeds are allowed to shade dried for several days. The completely dried seeds were then stored in airtight containers till the extraction of oil.

2.3. Chemical Oil Extraction

For oil extraction, seed samples were oven dried overnight at 60 °C. Then, 50 g of each non-edible feedstock's dry seeds were crushed into a fine powder using a mortar and pestle. Following that, the powder samples were placed in a Soxhlet apparatus (VWR VELP Scientifica, Darmstadt, Germany) equipped with a reflux condenser, a round bottom flask, and a thimble holder (Plate 2.1). Moreover, 250 mL of any solvent, such as n-hexane, was used for 7 h at a temperature of 65–70 °C to extract the oil [40].

To determine the oil content of seeds, the mean weight differences between the sample before and after chemical extraction were calculated. Three to five repeats of each experiment were conducted, and the mean values were used for further analysis. Following completion of the chemical extraction, the residual solvent was recovered using a rotary evaporator operating at 50 °C in a restricted vacuum condition. The oil content of the seeds was calculated by the following formula:

$$\text{Oil content (\%)} = \frac{W3(\text{weight of sample used}) \times W1(\text{Weight of empty flask})}{W2(\text{weight of empty flask} + \text{powdered sample})} \times 100 \quad (1)$$

where W3, W1, and W2 are used for weight of sample, empty flask, and powdered sample, respectively.

2.4. Mechanical Oil Extraction

The usage of mechanical presses is the most conventional approach to seed oil extraction. This method allows large amounts of oil mining from foodstuffs that are edible or not edible. In this study, oil was produced by electric oil expellers for experimental optimization (model KEK P0015, 10127, Remscheid, Germany). The seed cakes were passed through various presses to obtain a maximum amount of oil [41]. The crude oil extracted was kept in dried glass bottles to prevent photo-oxidation and self-oxidation [42].

2.5. Oil Filtration

The crude oil extracted from *C. colocynthis* feedstocks includes dust particles and other contaminants that can affect yield, quality, and rate of reaction. The oil extracted was filtered through Grade 2 (Plate 2 of Whitman), and for further analysis, the filtered oil was stored in airtight containers in the dark [43].

2.6. Free Fatty Acid (FFA) Content Determination

The free fatty acids (FFAs) found in the fatty oil sample are referred to as the fatty oil or biodiesel acid. The decay level of oil as a consequence of the thermal effect is demonstrated. The free acid or acid content has been calculated using AOCS-CD 3d-63 method [44]. Acid value is the number of milligrams of KOH necessary in 1 g of the crude sample to neutralize the free fatty acid. KOH with 0.5 wt percent concentration of analytical grade was mixed with 2-propanol in order to produce 0.1 molar KOH solution (iso-propanol). The solvent blend was made of toluene and iso-propanol equal proportions. The isopropanol was produced in 1.0 wt percent of phenolphthalein solution. Then, 2 mL of the phenolphthalein index were added to the 125 mL solvent mix and neutralized against the KOH solution until the end point or rosy color appeared. Next, 125 mL solvent solution in a conical flask was added to a known quantity of oil sample. The reaction mixed in the reaction appeared to 2 mL of phenolphthalein indicator. The volume of hydroxide potassium solution used before and after titration was reported. Acid value of seed oil is determined by employing the following formula:

$$\text{Acid value (mg } \frac{\text{KOH}}{\text{g}}) = \frac{(V_A - V_B) \times M \times 56.1}{W} \quad (2)$$

2.7. Preparation of Phyto-Nanocatalyst Using Oil Cake Waste (OCW) Extract

Seed oil cake that has been collected and thoroughly washed with distilled water to remove pollution and contaminants can be dried at room temperature. The dried bark was reduced to a fine powder. The extract was dissolved in 100 mL of distilled water. Extracts were boiled for 30 min at 40–60 °C and stirred for two hours. The solution's color changes from light brown to dark brown, indicating the formation of nanoparticles. The resulting solution was centrifuged at 1800 RPM for 20 min. To remove any remaining impurities, the pellets were washed in distilled water and then dried in a hot air oven set to 65 °C. The dried nanocatalytic of copper oxide was calcined for three hours at 300 °C to achieve a fine, crystalline nanostructure [45]. A distinct green phyto-nanocatalyst, copper oxide, was synthesized in this study using *C. colocynthis* oil cake extracts. SEM, XRD, FT-IR, and EDX were used to characterize the synthesized catalysts. Copper oxide-based phyto-nanocatalysts have also been efficiently employed for methyl ester synthesis. The utilization of plant extracts, especially metal-based nanoparticles for the synthesis of crude oil biodiesel, was evidenced as advantageous compared to the microbial process due to the exclusion of tedious cell culture management. Green synthesis of phyto-nanoparticles is biocompatible, safe and non-hazardous, sustainable, and environmentally friendly. Such nanoparticles have applications in biomedical and pharmaceutical industries, water electrolysis, optics and electronics, biosensors, bioimaging, tissue engineering, protein detection, and catalysis [1].

2.8. Synthesis of Biodiesel from Non-Edible Seed Oil via a Phyto-Nanocatalyst

The transesterification reaction was carried out in a three-necked circular bottom flask equipped with a magnetic stirrer and reflux condenser (250 mL). A three-necked round bottom flask was poured out and 25 mL of filtered seed oil was pre-heated to the correct temperature. After bringing the seed oil to a temperature of 65 °C, a variable amount of nanocatalyst (0.1–0.4 wt percent) and anhydrous methanol were added (with a ratio of 1:9–1:18). The reflux reaction was carried out at a temperature range of 90–180 °C to achieve a two-hour transactional reaction (Plate 8). When the reaction was complete, the catalyst was recovered via centrifugation, and the untreated methanol was recovered using a rotating vacuum evaporator at a temperature of 50 °C. A mechanism was transported to a separation funnel for carefully separating biodiesel and glycerol [46].

The yield of biodiesel was calculated using the following formula:

$$\% \text{ yield of biodiesel in 100 g} = \text{grams of oil used} \quad (3)$$

A series of research tests were performed in optimized conditions using synthesized green CuO and nanocatalysts to obtain the maximum rendering of biodiesel from non-edible seed oil.

2.9. Phyto-Nanocatalyst Characterization

2.9.1. FT-IR Spectroscopy (FT-IR)

In order to determine the spectroscopy of the mid-infrared emission and absorption spectroscopy of the synthesized phyto-nanocatalyst of copper oxide. In transmission mode the FT-IR spectra were recorded at a resolution of 4 cm^{-1} at $400\text{--}4000\text{ cm}^{-1}$ (PerkinElmer Spectrum 65).

2.9.2. Analysis of X-ray Diffraction (XRD)

The most used technical known as X-ray diffraction determines general crystalline properties of the nanoparticles. This analysis technique allows the nanocatalyst to detect its crystallite size and structure. The synthesized copper oxide and the nanocatalyst of aluminum were found to be XRD in shape and crystallite size.

2.9.3. Scanning Electron Microscopy (SEM)

The morphology and particle size of the synthesized phyto-nanocatalysts were determined using electron microscopy (SEM). Dispersed into dual distilled water and sounded 30 min in a 750 W Ultrasonic Processor for 10 mg/L of synthesized nanocatalyst (20 kHz) (Sonics Corp., Stratford, CT, USA).

2.9.4. Energy-Dispersive X-ray Analysis (EDX)

The EDX analysis reveals the presence of various metals and the elementary composition of synthesized nanocatalysts. The EDX study used EDX attachments from SEM (JOEL JSM-5910, Rock Hill, SC, USA).

2.9.5. Biodiesel Characterization

(a) GC-MS Analysis

The synthesized fatty acid methyl esters (FAMES) of various seed oil were characterized by a capillary column of SE-52 and EI detector with GC MS HP4890D (Little Falls, CA, USA). A fluctuating rate of 1.44 mUmin was used as the carrier gas. The column temperature was set at $90\text{ }^{\circ}\text{C}/\text{min}$ between 120 and $250\text{ }^{\circ}\text{C}$. The detector temp at $120\text{ }^{\circ}\text{C}$ and the injection port at $250\text{ }^{\circ}\text{C}$ have been adjusted.

(b) FT-IR Spectroscopy

The mid-infrared spectrum of emission and absorption of synthesized biodiesel is determined by the FT-IR spectroscopy. The measurements of absorption and emission by liquid cells were examined. The membrane method was used for liquid cell measurements.

2.10. Fuel Properties of Synthesized Biodiesel

The fuel properties of synthesized biodiesel were determined and compared to ASTM international standards in order to determine their qualitative characteristics. The cloud points (D-2500), total acid numbers (ASTM-D974), cinematically viscous at $40\text{ }^{\circ}\text{C}$ (ASTMD-445), flash points (D-93), pour points (ASTM-D97), and density at $15\text{ }^{\circ}\text{C}$ kg/L of synthesized biodiesel were determined in accordance with the standards (ASTM D-1298). Biodiesel must be also characterized by its higher heating value (HHV) and by lower heating value (LHV).

2.11. Experimental Design (Response Surface Methodology)

The trials were carried out using central composite design (CCD). The MINI-TAB 17 was used for the statistical analysis, and analysis of the variance (ANOVA) was used to optimize the experimental conditions. Utilizing a three-factor approach, the 17 experiments

were carried out to optimize the transesterification process. The three selection criteria for extraction are A: methanol–oil (mol), B: catalyst (%), and C: temperature (C). Randomization was used to lessen the effects of the mysterious variety in perceived responses. Following the conclusion of the studies, data were statistically analyzed by RSM to determine that the quadratic ploy approach appeared to be fitted using Design of Expert 11 (Stat-Ease Inc., Minneapolis, MN, USA). By modelling the dependent factor as y (yield) with the investigative factors A, B, and C, the reaction may be connected.

$$Y = b_0 + \sum_{i=1}^k b_i X_i + \sum_{i=1}^k b_{ii} X_i^2 + \sum_{i < j}^k b_{ij} X_i X_j + e \quad (4)$$

where Y and b₀ are the value of biodiesel yields (CTBD) and intercept values (e.g., 1, 2, 3 . . . , k), respectively.

3. Results and Discussion

3.1. Seed Characterization

C. colocynthis seeds are brown in color with clavate shape. Their compression is depressed and the helium is not visible. Surface ornamentation is rogues with bulging protuberance, cell arrangement is irregular and reticulate, apertures are absent, while anticlinal walls are thick and depressed, periclinal, and thick and elevated (Figure 1).

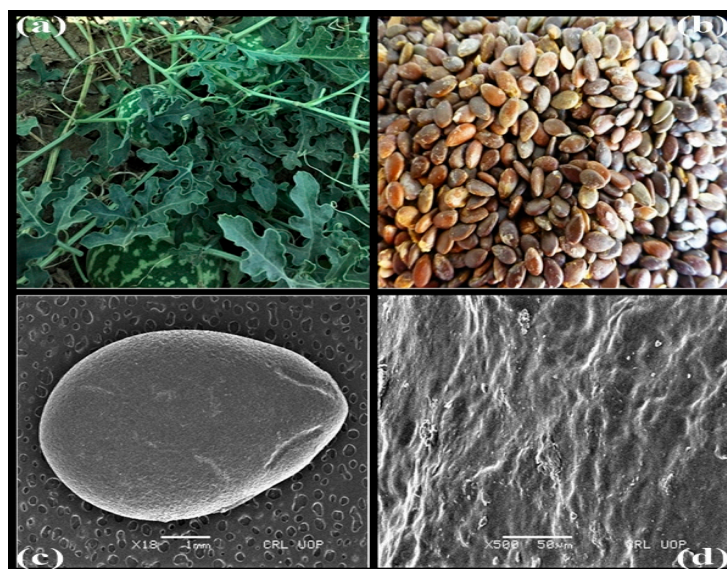


Figure 1. *Citrullus colocynthis* (L.) Schrad. (a) Entire plant, (b) seeds, (c,d) SEM micrograph of seeds and sculpturing.

3.2. Characterization of Green Nanocatalysts

3.2.1. (a) Characterization of Green Copper Oxide Nanocatalyst

The green CuO nanocatalyst has been selected for the present project because of its significant catalytic properties. The use of green nanoparticles for transesterification has been declared strong. The authors of reference [47] synthesized *Juglans regia* leaf extract green copper oxide particles and monitored their biological and oxide-related physical-chemical properties. Due to its catalytic and optic characteristics, green CuO has gained great importance [48]. By using *Phoenix dactylifera* leaf extract and observing the catalytic efficiency, the authors of [49] synthesized green copper oxide nanoparticles, biosynthesized *Drypetes sepia* leaf extract green copper oxide nanoparticles, and observed their catalytic activity for color degradation using X-ray diffraction analysis (XRD).

The XRD green nanocatalyst copper oxide spectrum is shown in Figure 2. The XRD spectrum includes several visibly distinguishable diffraction peaks. Different diffraction points at 2θ angles were observed (110), (002), (111), (202), (113), and plane orien-

tation for copper oxide was assigned (32.78, 39, 48.95; 53.92, 58.75, 61.79, 66.49, 68.29) (JCPDS 80-1268). There were no dominant peaks in other phases, which demonstrates the high purity of the product made using this method. The XRD-synthesized nanocatalyst copper oxide spectrum shows the particles in the mono-clinical phase to be in use. The average nanocatalyst of copper-oxide crystallite obtained from XRD is 34 nm calculated by $D = \lambda / \beta \cos \theta$ of Dybe–Scherrer. Biosynthesizing nanoparticles in *Drypetes* leaf extract and their XRD results from green copper oxide nanoparticles show the monoclinic structure with a mean crystalline size of 25 nm [49].

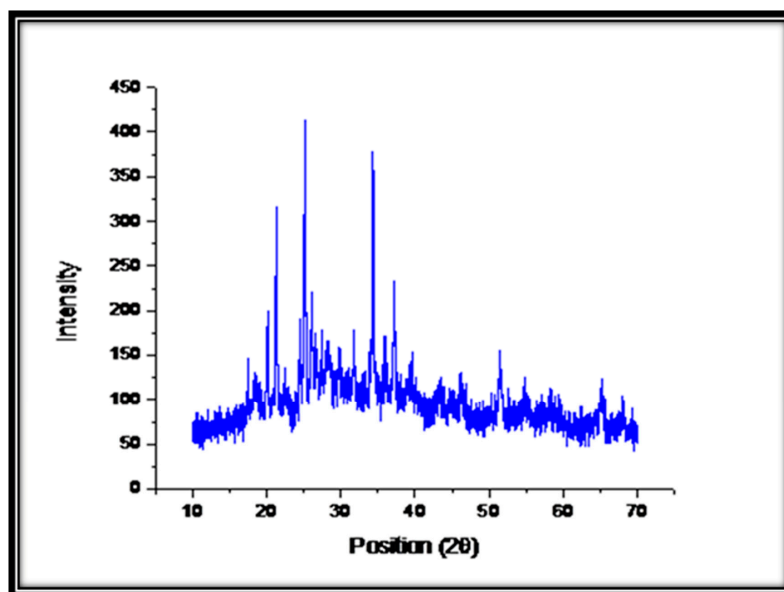


Figure 2. XRD pattern of calcined catalyst.

3.2.2. (b) Scanning Electron Microscopy (SEM) of CuNPs

Morphology of the surface of copper oxide at different lengths. SEM analysis revealed that copper oxide (CuO) nanoparticles are rod-like and agglomerate to form a smooth surface. The average nanocatalyst particle size for copper oxide was calculated to be between 80 and 85 nm. SEM results show a general a sphere surface design. Raul et al., (2014) [50] synthesized co-oxide nano rods and examined their surface morphology using SEM techniques, revealing an average rod-like surface pattern of 2.16 nm (Figure 3).

3.2.3. (c) FT-IR Spectroscopy of CuO NPs

The surface structural characteristics of the green synthesized CuO are investigated in the analysis of FT-IR and the data obtained are shown in Figure 4. The spectrum of saturated hydrocarbons, C-H, and carbonyl groups, which correspond to the green surfactant present on the surface of CuO NPs, revealed deepening and bending vibrational maxima. The stretching and bending viable of Alkenes (C=C-H) groups and aromatic groups could be a broad pin absorption of 3196.06 and 1422.75 cm^{-1} , respectively. At 1110.96 cm^{-1} , the strong extending bow shows the extension of the group (C-O-C) Alkyls or of the ether. The strong bending peaks at 683.86 and 600.01 cm^{-1} are shown at the spectrum, which reveals the characteristics of each functional group on the surface of CuO NPs which corresponds to bending vibrations for the C-S connection. Halogen compounds can be allocated to the other peaks at 600 and 500 cm^{-1} . C-O is an indicator of metal–oxygen bonds (Cu–O) in CuO NPs that confirms their chemical formation.

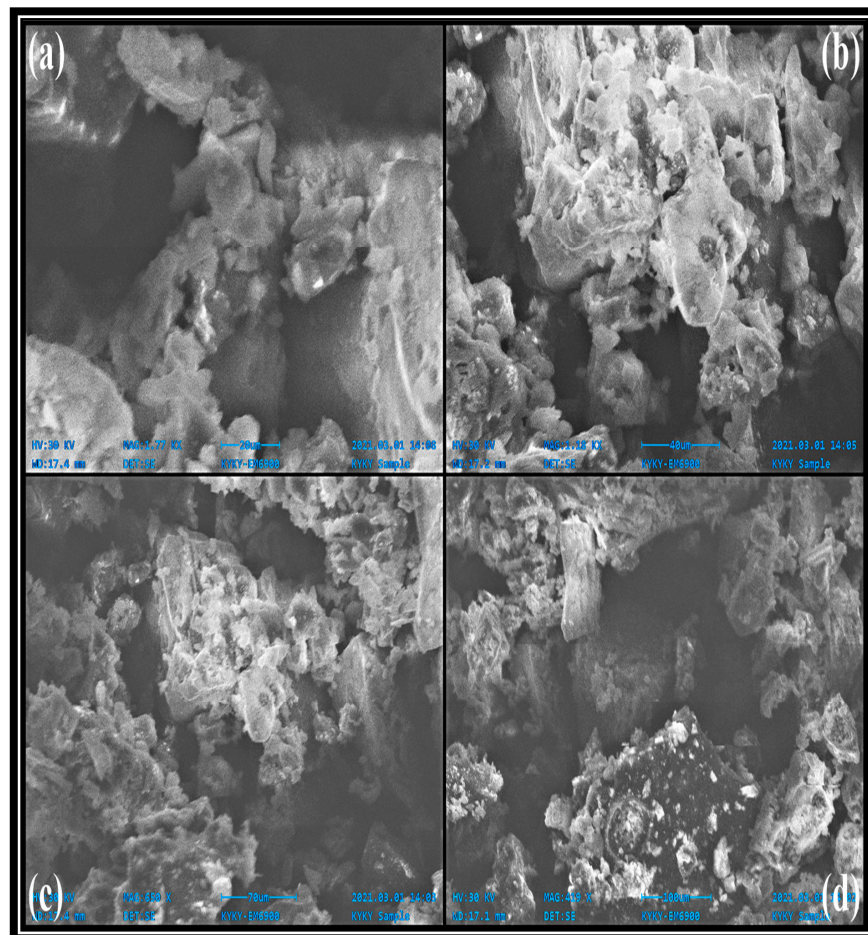


Figure 3. SEM microphotographs: (a–d) show different SEM visualized sculpturing elements of oil cake (OC)-based CuO catalyst.

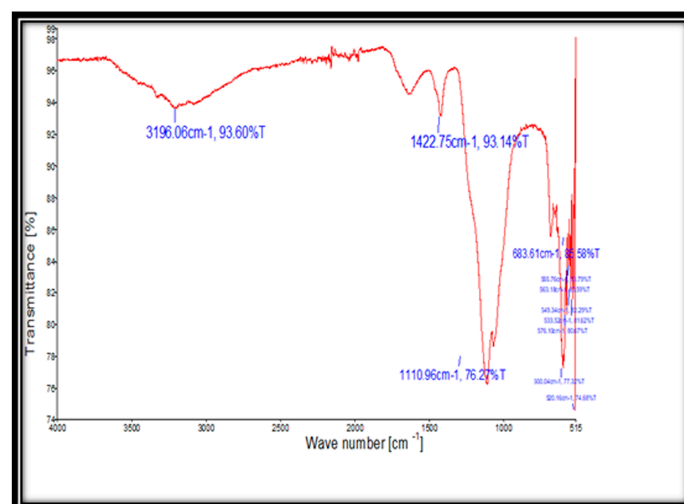


Figure 4. FT-IR spectra of catalyst.

3.2.4. (d) Energy-Dispersive X-rays (EDX)

The composition of elements in oil cake waste of seed (OCW)-based catalyst has been verified via EDX as shown in Figure 5. EDX copper oxide (CuO) phyto-nanocatalyst analysis clearly reveals that those two different elements (i.e., copper and oxygen) were composed of synthesized phyto-nanocatalyst as shown in Figure 5. Several typical points

have been selected on the catalyst surface. The peaks similar to the optical absorption of the produced nanocatalyst have been determined by EDX analysis. The basic analytical results for nanocatalysts showed that the synthesized phyto-nanocatalyst is in its highest purification state in addition to the nanocatalyst recommended for the proposed catalysis of triglycerides into fatty acid esters, 77.62% copper and 21.54% of oxygen and some minor residue of potassium K (0.84%). The purity of their biosynthesized CuO NPs were determined in EDX analysis. By using *Ixora coccinea* leaf extract, they synthesized ZnO nanoparticles and found that their elementary analysis was 78.6% copper and 19.8% oxygen [51]. Hence, all results are close according to previous research.

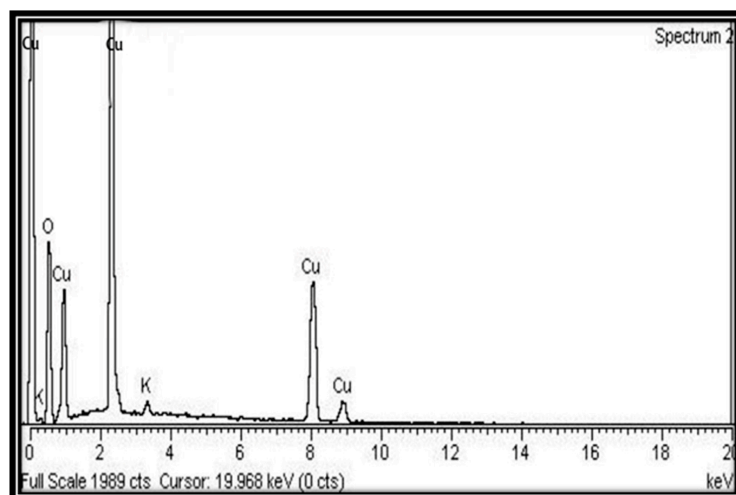


Figure 5. Energy-Dispersive X-ray of calcined oil cake (OC)-based CuO.

3.3. Biodiesel Synthesis and Characterization

The synthesized CuO Nps catalyst provides 95.42% biodiesel (CTBD) during two-step transesterification of CPSO with 1:8 oil:methanol, 0.25% catalyst amount at 80 °C for 2 h. The CTBD was then characterized using different techniques.

3.3.1. (a) FT-IR Analysis of CTSO and CTBD

FT-IR is an efficient and fast approach for analyzing the formation of FAME after the transesterification reaction has already been completed [52]. FT-IR spectroscopy was used to detect formation of fatty acid methyl esters (FAMES) after transesterification as an accurate technique. A clear indicator of their corresponding methyl ester is CTBD FT-IR spectrum using CCSOC (*C. colocynthis* seed oil cake, CuONPs (Figure 6). Various bands of synthesized biodiesel were detected in the spectrum representing different functional groups. *C. colocynthis* seed oil and biodiesel spectra are presented in Figure 6 in the mid-IR region (400–4000 cm^{-1}). CTSO and CTBD spectra (Figure 6) do not appear very similar, with differences in band intensity and absorption rates possibly due to differing oils and biodiesel characteristics. Alcohols are present at the important peak observed in 3279.16 cm^{-1} (O-H stretch). The peaks are attributed to Alkanes, albeit at 2928.26 cm^{-1} ($\text{sp}^3\text{C-H}$ stretch). In contrast, the Aldehydes represent a peak of 2848.10 cm^{-1} ($\text{sp}^2\text{C=O}$ stretch). The ester keto-enol peak is 1643.12 (C=O stretch). The result of Alkenes can be seen in the other peak at 1554.65 cm^{-1} (C=C stretch). Alkyl halides and aryl halides were attributed to the peak of 1405.77 cm^{-1} (spreading bend for ester group). R1-C (OR) = O for the oil group, whereas R1-C (OCH₃) = O for the bio-diesel group. This can be called R1-C (OR). The peaks show the bent vibrations of CH₂ and CH₃ in biodiesel and oil, respectively, and 1464, 1377, and 1089, but also 1112 and 1014 cm^{-1} (C-O primary and secondary alcohol stretches are the confirmation of the esters). At 1236 cm^{-1} , which is absent in seed oil spectrums, the highest elevation of the biodiesel conversion of methyl ester is found. The ester control signal is shown at another 1112 cm^{-1} peak. There is a

powerful, broad signal in CTSO at 1743 cm^{-1} and 1643 cm^{-1} (signal strong) (Figure 6). The peak shows a $-\text{CH}_2$ wagging for oils, which is not present in biodiesel spectra at 1743 cm^{-1} , 1464 cm^{-1} , 1377 cm^{-1} , 1236 cm^{-1} , and 1159 cm^{-1} . The confirmation of biodiesel formation shows all related justifications in the above texts and pits.

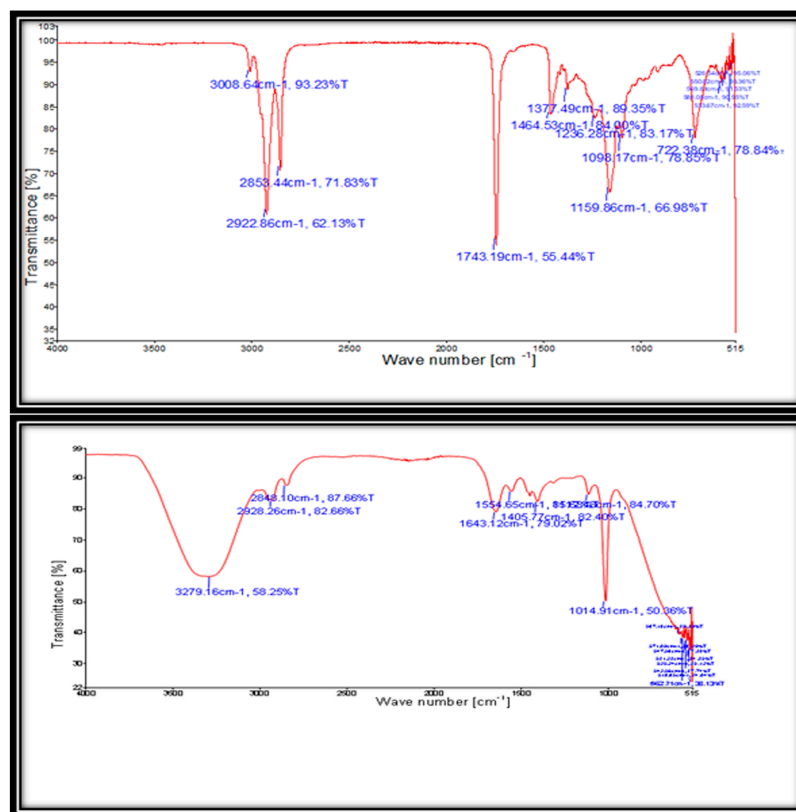


Figure 6. FT-IR spectrogram of *C. colocythis* seed oil (CTSO) upper and *C. colocythis* biodiesel (CTBD) lower.

3.3.2. (b) GC-MS Analysis of CTBD

The most widely used and highly acceptable method for identification of the structure, chemical design, or fatty acid methyl esters (FAMES) is gas chromatography and mass spectroscopy. In the gas chromatogram in Figure 7, the chemical structure of methyl ester in CTSOB can be seen. Several peaks in the gas chromatogram have been observed and further determined by matching them with the NIST library 11 standardizations in the manufactured biodiesel that agree with the FAMES.

The resulting hierarchy shows the effectiveness of green nanocatalysts, i.e., copper oxide, in the production of biodiesel. The methyl esters that were synthesized by green nanocatalysts are 65.55%. Due to its specific, high surface area and small particle size, the catalytic competence of the copper oxide was maximal. Catalyzed CTSOB GC-MS copper oxide spectrum showed six significant peaks, each corresponding to one single fatty acid ester that was further confirmed by the NIST library 11 match software. The most important FAMES are ethane,1,2,2-trichloro-1,1-difluoro, 9,12-ocadienoic acid (Z, Z), metal (C18:2). Table 1 shows the retention time of the determined fatty acid methyl esters and FAMES have been identified by tracing data on retention time; in addition, internal GC standards have been verified.

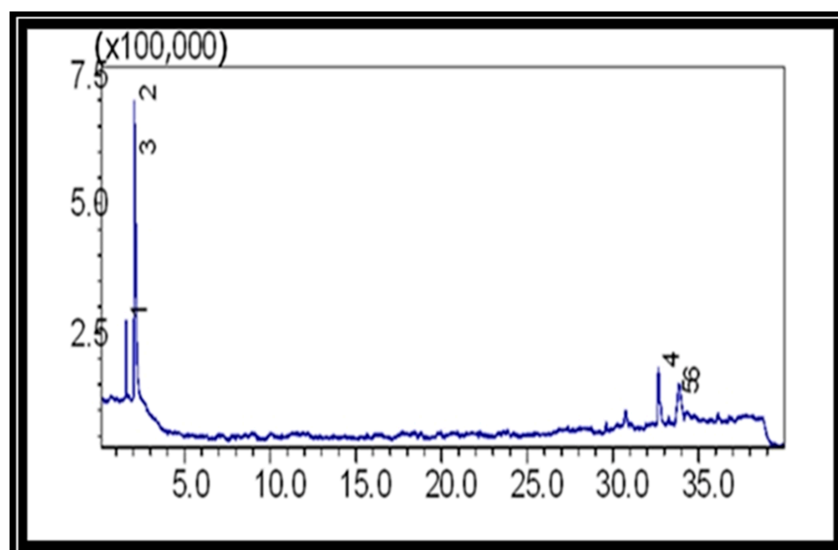


Figure 7. GC-MS spectrogram of *C. colocynthis* biodiesel.

Table 1. Properties of crude *C. colocynthis* seed oil (CTSO).

S. No.	Property	CTSO
1.	Acid Strength mg KOH/g	0.110
2.	Saponification Number (mg KOH/g)	118.15
3.	Iodine Strength (g)	60.45
4.	FFA Concentration (%) <i>w/w</i>	1.68
5.	Percentage of oil (%)	29

3.4. Physico-Chemical Properties of *C. colocynthis* Seed Oil (CTSO)

Prior to converting it to biodiesel, it is important to determine the content of the *C. colocynthis* (CTSO), which, together with free fatty acid [53], is found to be significantly higher in RRSO oil content (29%) based on dry biomass [54]. However, the potential oil yardstick for biodiesel synthesis has not previously been explored. *C. colocynthis* seed oil is imminently expected to be a supplier to the biodiesel industry in this respect. The determination of physico-chemical properties is extremely important when assessing the quality of the understudies' oil. At the acid value of 0.110 mg/KOH acid, oil was blackish brown at normal temperature ($^{\circ}\text{C}$). Table 1 shows other CTSSO parameters. However, low CTSSO FFA values (1.68 mg/KOH and 0.80 mg/NaOH) show that yield, quality, and synthesis of biodiesel are directly influenced. In addition, the FFA's optimal value of 3% is ideal for the synthesis of biodiesel [55]; values higher than that would lead to steady reduction in conversion into undesirably products (saponification) and snags in finished product segregation [56].

3.5. Transesterification Optimization of Operational Factors Using the Response Surface Methodology (RSM)

For transesterification optimization process, four independent variables (methanol oil (A) 2:1–10:1, (B) catalyst 0.48–0.8%), (C) reaction temperature 50–120 $^{\circ}\text{C}$, and (D) time 1–3 h have been chosen and a central composite design (CCD), applied to 30 experiments to test quadratic fitness (Table 2). A central composite design (CCD) was used to determine the fitness of a transesterification process (Stat-Ease Inc., Minneapolis, MN, USA). A coded model equation was used below to represent the input variables (methanol oil (A), catalyst (B), temperature (C), and time (D), as well as the output response in terms of yield (Y) given below:

$$\text{Yield} = +80.32 + 5.06A1.20B + 1.96C + 2.68D + 1.76AB + 1.11AC + 1.13AD + 0.9375BC - 0.3125 BD - 0.0625CD - 16.38A2 + 10.71B2 + 2.21C2 - 14.29D2$$

Table 2. *C. colocythis* biodiesel (CTBD) with CCD experimental and predicted yield (central composite design).

Run	Factor 1	Factor 2	Factor 3	Factor 4	Response 1
	A: Alcohol-to-Oil Molar Ratio	B: Catalyst Loading wt%	C: Reaction Time Min	D: Temperature °C	Yield %
1	3.1	0.48	180	120	60
2	8.1	0.365	60	85	70
3	8.1	0.365	120	85	85
4	3.1	0.25	60	50	65
5	14.1	0.25	60	120	68
6	14.1	0.25	60	50	62
7	8.1	0.25	120	85	95
8	8.1	0.365	120	120	70
9	8.1	0.365	180	85	88
10	14.1	0.48	180	120	67
11	8.1	0.48	120	85	80
12	14.1	0.48	180	50	77
13	14.1	0.48	60	50	62
14	8.1	0.365	120	85	85
15	8.1	0.365	120	50	55
16	3.1	0.25	180	120	58
17	3.1	0.25	180	50	60
18	3.1	0.25	60	120	58
19	3.1	0.48	60	50	50
20	3.1	0.48	180	50	54
21	14.1	0.25	180	120	79
22	14.1	0.48	60	120	70
23	8.1	0.365	120	85	87
24	8.1	0.48	120	85	70
25	14.1	0.365	120	85	68
26	3.1	0.48	60	120	60
27	14.1	0.25	180	50	57
28	8.1	0.365	120	85	83
29	3.1	0.365	120	85	54
30	8.1	0.365	120	85	86

The ANOVA results in Table 3 contribute to the enhancement of biodiesel production (methyl esters). The model's F-value and corresponding lack of fit were used to determine the model's significance. The significance of F-value 3.98 (p -value 0.05) is that it corresponds to the lack of fit (1.82) and thus demonstrates the optimum fitness of models with

experimental (trial) data, which appears to be unrelated to the corresponding pure error. The produced biodiesel yield ($R^2 = 0.7880$) exhibits 96.59 percent variability, indicating the model's reliability. The signal-to-noise ratio measurement is precise, and the value obtained (7.236) exceeds 4, implying that biodiesel output is estimated. The only difference (0.2) between the adjusted R^2 ($R^2 = 0.5902$) and the R^2 value ($R^2 = -0.0702$) is the R^2 value ($R^2 = -0.0702$), indicating the polynomial regression's high correlation.

Table 3. Analysis of variance (ANOVA) on the obtained data.

Source	Sum of Squares	df	Mean Square	F-Value	p-Value	
Model	3465.29	14	247.52	3.98	0.0059	significant
A-Alcohol-to-oil molar ratio	460.06	1	460.06	7.40	0.0158	
B-Catalyst loading	26.11	1	26.11	0.4202	0.5266	
C-Reaction time	68.83	1	68.83	1.11	0.3092	
D-Temperature	129.08	1	129.08	2.08	0.1700	
AB	49.45	1	49.45	0.7958	0.3864	
AC	19.60	1	19.60	0.3154	0.5827	
AD	20.50	1	20.50	0.3300	0.5742	
BC	14.06	1	14.06	0.2263	0.6411	
BD	1.56	1	1.56	0.0251	0.8761	
CD	0.0625	1	0.0625	0.0010	0.9751	
A ²	683.27	1	683.27	11.00	0.0047	
B ²	297.22	1	297.22	4.78	0.0450	
C ²	12.66	1	12.66	0.2037	0.6582	
D ²	529.04	1	529.04	8.51	0.0106	
Residual	932.08	15	62.14			
Lack of Fit	730.75	10	73.07	1.81	0.2650	
Pure Error	201.33	5	40.27			
Cor Total	4397.37	29				
Standard deviation	7.88		Adjusted R ²	0.5902		
Mean	69.43		Predicted R ²	-0.0702		
Co-efficient of variation	11.35%		Adequate precision	7.2360		
R ²	0.7880					

Additionally, the p value (Table 3) is less than 0.05, defining terms such as A (oil ratio methane), B (catalyst quantity), C (process temperature), D (process time), AB (oil ratio and catalyst quantity methanol), AC (oil and temperature methane oil ratio), AD (oil/time methanol), BC (catalyst quantity and temperature), and BD (catalyst quadratic impact of reaction time) [57].

3.6. Parametric Characterization of Transesterification Process for Biodiesel Yield

The three-dimensional response curves in Figure 8a–f (3D) plot versus any dual variable, with another variable pivotal. The following sections explain the interactive effects of a transesterification reaction.

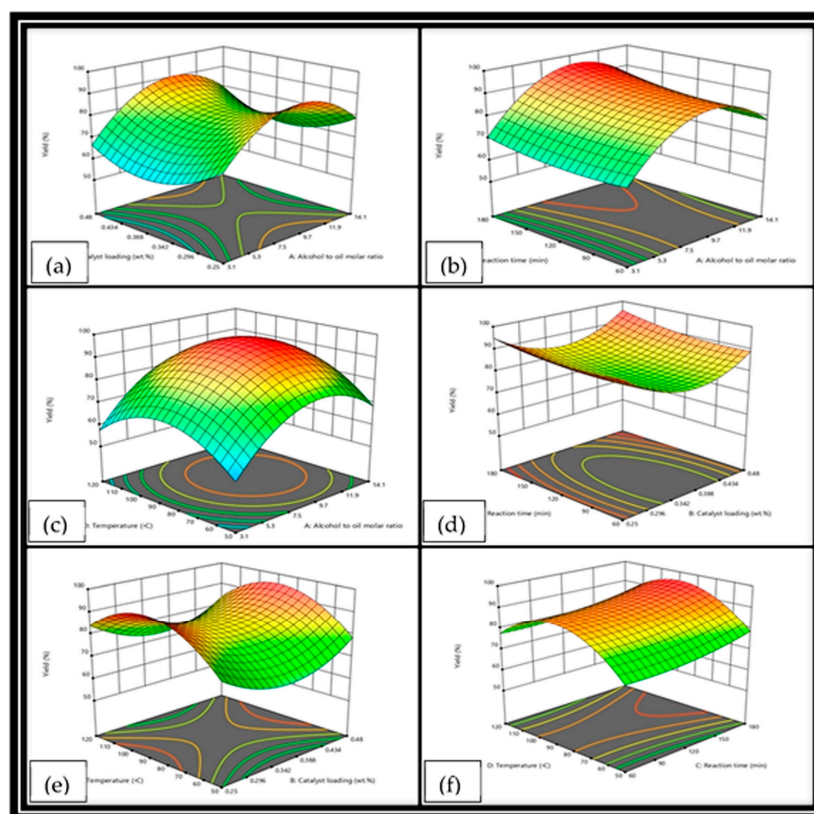


Figure 8. 3D plots showing impact of different reaction parameters on biodiesel yield: (a) 3D surface illustrating combined effect of oil-to-methanol ratio and catalyst, (b) catalyst charge by 0.25% and the temperature of reaction by 85 °C, (c) oil-to-methanol conversion results and reaction temperatures for final biodiesel production, (d) combined effect of reaction times and catalyst quantities on biodiesel yield, (e) combined effect of temperature and catalyst concentration on biodiesel yields, (f) interaction between reaction time and temperature on biodiesel yield.

3.6.1. Collective Impact on Biodiesel Yields of Oil: Methanol and Catalytic Changes

Using CCD experimental design parameters, Figure 8a depicts a three-dimensional surface graph illustrating the combined effect of oil-to-methanol ratio and catalyst loading on biodiesel production rates. The highest biodiesel yields were achieved using a 0.25% catalyst and a ratio of 1:8 of oil to methanol (95%) (Run 7). If the oil-to-methanol ratio in catalyst increases by 0.48% constantly, the biodiesel return is reduced to 80% (Run 11). This is because the increased catalyst concentration promotes unwanted product development (soap formation). Furthermore, the biodiesel net yield is 50 percent by decreasing the ratio of oil to methanol to 1:3 with a catalyst increase of 0.48% (Run 19). The ratio of oil to methanol is an essential factor in the production of biodiesel. Moreover, 3 moles of methanol is required for stoichiometric transesterification of oil (1 mole) to produce glycerol (1 mole) and biodiesel (3 mol). Additional methanol is required to advance the reaction due to the double-sided transesterification. By contrast, the rate of oil-to-methanol conversion increased to 1:14 and a catalyst concentration of 0.48 wt% reduced biodiesel production to 62 percent. (Run 13). This decrease in biodiesel yield (62%) is due to glycerolizing (reversible reaction). The reversible reaction is caused by monoglycerides, which promote the mixing and solubility of glycerol in FAME. This makes it easier to recombine FAME with glycerol, which results in the formation of monoglycerides, which reduces biodiesel output by 62% when the oil–methanol ratio is increased to 1:14.

The results are consistent with previous research, which indicates that providing an excessive amount of methanol for reversible effects reduces final biodiesel production. In the current study, increased methanol concentrations also impede glycerol separation,

contributing to the lower FAME rating. However, the ANOVA data demonstrated that the combined effects of oil–methanol and catalyst concentration have a p -value (0.3868) > 0.05 .

3.6.2. Collective Effects on Yields of Biodiesel from Oil to Methanol and Reaction Time

The collective effects of oil on methanol and reaction times are shown in Figure 8b, maintaining other constant parameters such as catalyst charge at 0.25% and the temperature of reaction at 85 °C. The highest biodiesel yield of 95% was attributed to the increased interaction between excessive alcohols and oil in Run 7 due to the oil-to-methanol ratio of 1:8 and the reaction time of 2 h. In contrast, in Run 18, a shorter reaction time of 1 h combined with a lower oil/methanol ratio of 1:3 results in a partial conversion of reactants to the equilibrate stage during the given period. Strong reaction time effects on biodiesel production from rice oil have been confirmed. There was a slight decrease in biodiesel yield (79%) with a reaction time of 3 h and a ratio of 1:14 oil to methanol in Run 21, where increasing the methanol changes the reaction in the direction of the adverse condition to obtain the desired biodiesel yields.

3.6.3. Collective Effects of Methanol Oil: Reaction Temperature

The combined oil-to-methanol conversion results and reaction temperatures for final biodiesel production are shown in Figure 8c. With the reaction temperature increased to 85 °C and 8 mL of methanol added to the reaction medium, a 95% yield of biodiesel was obtained (Run 7). However, as the temperature threshold exceeds 85 °C, the output of biodiesel decreases significantly (70% Run 8). Because the oil, methanol, and Cu nanoparticles are invisible, the mass transfer rate has been reduced. Thus, increasing the temperature to a certain point (85 °C) aids in mass transfer between these two immiscible phases (oil, methanol, and Cu-oxides) by providing reactant molecules with additional kinetic energy, resulting in increased FAME yields in shorter reaction times. However, the yield increases with increasing molar ratio reaction temperature, but this increase in biodiesel yield is limited by the boiling point of methanol (65 °C). When the reaction temperature exceeds 85 °C, the output decreases. Saponification of glycerin occurs prior to methanol decomposition, lowering the biodiesel yield as the temperature rises above the methanol boiling point. As a result of the results obtained, it can be concluded that the combined effect of reaction temperature and oil-to-alcohol ratios (p value = 1.446E + 05 0.05) is highly significant, which is inconsistent with previously published work.

3.6.4. Collective Effects on Biodiesel Production of Reaction Time and Catalyst Loads

The combined effect of reaction times and catalyst quantities on biodiesel yield, while keeping other parameters such as the 1:8 oil-to-methanol ratio and the reaction temperature of 85 °C constant, is shown in Figure 8d. At the optimal catalyst charge and process time, the maximum biodiesel yield of 87% was achieved due to reaction equilibrium (0.365%, 2 h). Along with the optimal catalyst concentration and reaction time (0.48%, 3 h), a sudden drop in output (77%) was observed, similar to the work reported. Even with a higher catalyst concentration, a shorter reaction time does not favor completion (Run 13) (62%). Long reaction times (Run 27) and a catalyst concentration of 0.25% also contribute to reversible transesterification, which results in decreased biodiesel production. The current study's parameters are not significant because the p -value (0.6411) is greater than 0.05 for the transesterification reaction.

3.6.5. Collective Effect on Biodiesel Output of the Reaction Temperature and Catalyst Loads

The combined effect of temperature and catalyst concentration on biodiesel yields is shown in Figure 8e. The maximum biodiesel output (95%) was achieved in Run 7 with a catalyst loading of 0.25 wt% and a reaction temperature of 85 °C. However, with a 0.25% catalyst and 60 °C reactions, a lower biodiesel conversion (62%) was observed (Run 6). When the catalyst concentration and reaction temperature are increased above 0.25% by

weight (Run 8) and 85% by weight, similar yield drops of 70% are observed (Run 7). This decreased biodiesel yield is a result of the reaction mixture's increased viscosity due to the addition of catalyst. Our findings are consistent with previous research. As a result of the ANOVA results, the interactive effect of catalyst concentration and temperature is insignificant, with a p -value of 0.8761, greater than 0.05.

3.6.6. Effect of Reaction Time and Temperature on Biodiesel Yields

The interaction between reaction time and temperature on biodiesel yield is depicted in Figure 8f. Run 7 indicates that yield increased (95%) as temperature and catalyst concentration increased to a maximum of 85 °C, and that further temperature and time increases (120 °C, 3 h) resulted in a decline in yield (67%). The Arrhenius equation may account for the increase in biodiesel yield and reaction rate associated with increasing process temperature. Consistent with previous research, our findings indicated that biodiesel yield increased until a certain temperature was reached and then decreased. This decrease in biodiesel yield is caused by the endothermic transesterification reaction.

The thorough mixing of oil and methanol, as well as the separation of glycerol and product, resulted in a maximum biodiesel yield of 95% at 85 °C and a reaction time of 2 h. Increased temperatures and time (Run 16) could result in an increase in the hydrolysis of alkyl esters to form acids, reducing biodiesel yield. As a result, reaction time and temperature have little effect on the final biodiesel yield (p -value = 0.9751 > 0.05).

3.7. *C. colocynthis* (CTBD) and the Resulting Fuel Properties Were Compared to International Standards

The fuel properties of CTBD synthesized under optimal reaction conditions are listed in Table 4, along with a comparison to North American (ASTM D-6751), European (ASTM D-951), and European Union (ASTM D-14214) biodiesel standards. The CTBD acid value (0.140 mg KOH/g) in Table 4 meets international standards (ASTM-D6751, 951, EN-14214, and PRC-GB-T 20828).

Table 4. Comparison of *C. colocynthis* (CTBD) biodiesel fuel properties to PRC-GB/T (20828), ASTM D-951, American (ASTM D-6751), and European standards (EN-14214).

Fuel Properties	Testing Method	ALM-B100 (Present Study)	ASTM Standards (D6751)	EN-12214	HSD ASTM D-951	China GB/T 20828-2007
Color	Visual	2.5	2	-	2.0	-
Flash point °C (PMCC)	ASTM D-93	73.5	>90	>120	60–80	≥130
Density @ 15 °C Kg/L	ASTM D-1298	0.810	<120	<120	0.8343	-
K. Viscosity @ 40 °C c ST	ASTM D-445	4.23	1.9 to 6.0	3.4–5.0	4.223	-
Pour point °C	ASTM D-97	−8	−15 to −16	-	-	-
Cloud point °C	ASTM D-2500	−4	−3 to 12	-	-	-
Sulfur wt%	ASTM D-4294	0.0000	<0.05	0.020	0.05	≤0.05
Total Acid No. mg KOH/g	ASTM D-974	0.110	<0.5	<0.5	0.8	≤0.8

3.7.1. Color

Visual color is somewhere between 2.5 and 3.

3.7.2. Density (kg/L)

Fuel density gives us an idea of the fuel's purity and free fatty acid amount, which is closely linked to the number of carbon atoms. Fuel concentrations that are high would cause viscosity issues in the engine. Meeting international standards (shown in Table 4), CTBD was found to be a suitable substitute fuel for diesel engines, with no harm to the environment or diesel engines.

3.7.3. Acid Number (KOH/g)

A large amount of free fatty acid is associated with an elevated acid value. Acid-rich mixtures can corrode engines and affect their performance. International standards that have been set establish the accepted value of the determined acidity of CTBD at 0.110 mg KOH/g. This value is too low, and it is suitable for commercial and mainly for transport use.

3.7.4. Flash Point (°C)

It is the degree of affinity of the substance in question to support the ignition of oxygen when present. The strong effect of methanol levels in synthesized biodiesel is an important feature [58]. The belief was that biodiesel with a higher flash point value (≥ 66 °C) was less dangerous during transport. The 73.5 °C CTBD flash point meets international standards.

3.7.5. Kinematic Viscosity (°C)

Kinematic viscosity plays an important role during combustion, as well as during the formation of blends and spray fuel. Operational difficulties such as engine deposits and incomplete combustion can be produced by high viscosity of fuel. Results of the current study show that the K. viscosity of CTBD is 4.23 at 40 °C, and these findings support the results of previous studies.

3.7.6. Pour Point and Cloud Point (°C)

The biodiesel quality is also dependent on the pour and cloud point. The temperature decreases, causing the biodiesel to turn milky as nuclei crystals begin to form and the fluid flowing ability is obstructed.

The temperature at which crystals begin to form is known as the cloud point [59]. It is highly probable that in cold weather, the diesel engine would be able to operate as long as the cloud point and pour point are both reached. The cloud point is subject to various factors, especially the types and quantities of impurities in the biodiesel sample. Possible use of additives and antioxidants is augmented by a small but significant increase in pour point (-8 °C) and cloud point (-4 °C).

3.7.7. Sulfur Content

According to our data, biodiesel contains no sulfur. The sulfur content of CTBD biodiesel was determined to be 0.0000 percent by ASTM D-4294 standards.

3.8. Catalyst Reusability

After the end of the reaction, heterogeneous (solid) catalysts can be easily reprocessed. Catalytic activity decreases, however, in connection with active sites' catalyst end product that reduces the catalyst reaction on methanol's surface. The feasibility and usefulness of the Cu-OC (oil cake-based) catalyst in the process of transesterification can be checked by examining its biodiesel reusability and operational parameters to obtain an optimized yield. Copper is shown in Figure 9. Catalyst reusability based on oil cake waste of seeds under optimal conditions (0.48% catalyst) (1:6 oil-methanol at 150 °C for 3 h). Catalysts at the end of each cycle of methanol and oven have been washed dry for up to 3 h (100 °C). The processed and washed catalysts were active and could be used three times more effectively without reducing their catalyst activity. On the other hand, there was a significant decrease in its activity during the catalyst's fourth cycle, which may be attributed to deactivation of the active site.

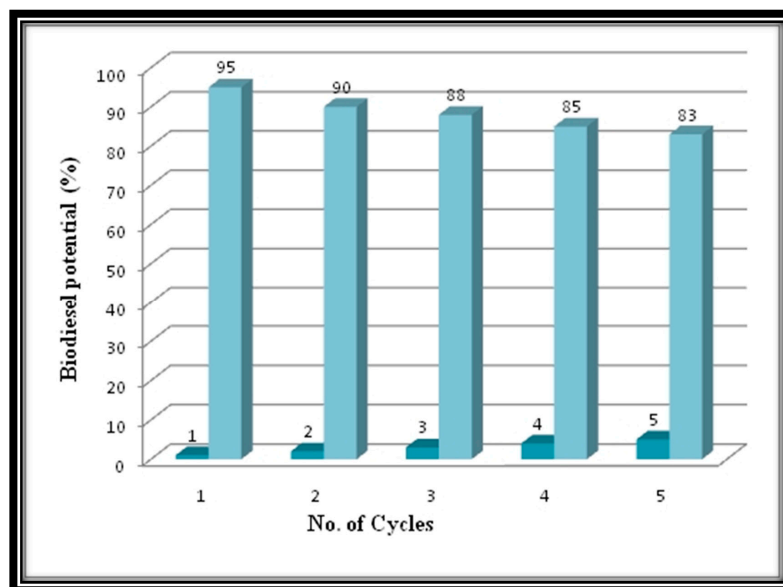


Figure 9. Reutilization of CuO phyto-nanocatalyst through transesterification.

4. Conclusions

The results of this study indicated that scanning electron microscopy may be a valuable tool for revealing hidden micromorphological characteristics in non-edible oil-producing seeds, thereby assisting in accurate, authentic seed identification and classification as a potential biodiesel feedstock. Prior to subjecting all non-edible seeds to the transesterification reaction that produces biodiesel, their physicochemical properties were determined. The results indicated that the *C. colocynthis* seed oils tested had an acidity of less than 3%. The distinct stable and inexpensive catalysts (CuO) were synthesized using the in situ wet impregnation method from seed oil cake waste. The activity of these catalysts was determined using response surface methodology during the transesterification of seed oil to biodiesel under optimized conditions. Optimal conditions for *C. colocynthis* seed oil (CTSO) production using Cu-O OCW particles were 1:8 oil-to-methanol ratio, 0.25 wt% catalyst concentration, and 85 °C for 2 h, yielding a maximum of 95% biodiesel (CTBD). Based on these experimental findings, it is economically possible to use the feedstock used in this project as raw material for commercial mass production.

Author Contributions: Conceptualization, A.A., Supervision, M.A. (Mushtaq Ahmad), Review editing, M.Z., Methodology, M.N., Software, A.-R.Z.G., Validation, M.S.H., Formal analysis, S.S., Investigation, M.A. (Mohammad Athar), Editing and Formatting, S.M., Data curation, F.A.O. and A.Y., Writing—original draft preparation, A.A., Writing—review and editing, T.M. and O.M., Statistics, S.M., Review first draft, B.C. All authors have read and agreed to the published version of the manuscript.

Funding: Grant Number (RSPD2023R686) King Saud University, Riyadh, Saudi Arabia.

Data Availability Statement: The data presented in this work are available on request.

Acknowledgments: The authors extend their appreciation to the researchers supporting project number (RSPD2023R686), King Saud University, Riyadh, Saudi Arabia.

Conflicts of Interest: The authors declare no conflict of interest.

Abbreviations

CCD = central composite design; CuNPs = copper nanoparticles; CTSO = *Citrullus* seed oil; CTBD = *Citrullus* biodiesel; EDX = energy-dispersive X-ray; FFA = free fatty acid; FT-IR = Fourier-transform infrared; GC-MS = gas chromatography–mass spectrometry; OCW = oilcake waste; RSM = response surface methodology; SEM = scanning electron microscopy; XRD = X-ray diffraction.

References

1. Ameen, M.; Zafar, M.; Ahmad, M.; Ramadan, M.F.; Eid, H.F.; Makhkamov, T.; Yuldashev, A.; Mamarakhimov, O.; Nizomova, M.; Isaifan, R.J. Assessing the Bioenergy Potential of Novel Non-Edible Biomass Resources via Ultrastructural Analysis of Seed Sculpturing Using Microscopic Imaging Visualization. *Agronomy* **2023**, *13*, 735. [[CrossRef](#)]
2. Akhtar, M.T.; Ahmad, M.; Ramadan, M.F.; Makhkamov, T.; Yuldashev, A.; Mamarakhimov, O.; Munir, M.; Asma, M.; Zafar, M.; Majeed, S. Sustainable production of biodiesel from novel non-edible oil seeds (*Descourainia sophia* L.) via green nano CeO₂ catalyst. *Energies* **2023**, *16*, 1534. [[CrossRef](#)]
3. Sankaranarayanan, A.C.; Studer, C.; Baraniuk, R.G. CS-MUVI: Video compressive sensing for spatial-multiplexing cameras. In Proceedings of 2012 IEEE International Conference on Computational Photography (ICCP), Seattle, WA, USA, 28–29 April 2012; pp. 1–10.
4. Jacobson, V.; Smetters, D.K.; Thornton, J.D.; Plass, M.F.; Briggs, N.H.; Braynard, R.L. Networking named content. In Proceedings of the 5th International Conference on Emerging Networking Experiments and Technologies, Rome, Italy, 1–4 December 2009; pp. 1–12.
5. Correa, D.F.; Beyer, H.L.; Fargione, J.E.; Hill, J.D.; Possingham, H.P.; Thomas-Hall, S.R.; Schenk, P.M. Towards the implementation of sustainable biofuel production systems. *Renew. Sustain. Energy Rev.* **2019**, *107*, 250–263. [[CrossRef](#)]
6. Hanssen, S.V.; Steinmann, Z.J.; Daioglou, V.; Čengić, M.; Van Vuuren, D.P.; Huijbregts, M.A. Global implications of crop-based bioenergy with carbon capture and storage for terrestrial vertebrate biodiversity. *GCB Bioenergy* **2022**, *14*, 307–321. [[CrossRef](#)] [[PubMed](#)]
7. Goh, B.H.H.; Chong, C.T.; Ge, Y.; Ong, H.C.; Ng, J.-H.; Tian, B.; Ashokkumar, V.; Lim, S.; Seljak, T.; Józsa, V. Progress in utilisation of waste cooking oil for sustainable biodiesel and biojet fuel production. *Energy Convers. Manag.* **2020**, *223*, 113296. [[CrossRef](#)]
8. Kaur, M.; Ali, A. Lithium ion impregnated calcium oxide as nano catalyst for the biodiesel production from karanja and jatropa oils. *Renew. Energy* **2011**, *36*, 2866–2871. [[CrossRef](#)]
9. Maddikeri, G.L.; Pandit, A.B.; Gogate, P.R. Intensification approaches for biodiesel synthesis from waste cooking oil: A review. *Ind. Eng. Chem. Res.* **2012**, *51*, 14610–14628. [[CrossRef](#)]
10. Sanjid, A.; Masjuki, H.; Kalam, M.; Rahman, S.A.; Abedin, M.; Palash, S. Impact of palm, mustard, waste cooking oil and Calophyllum inophyllum biofuels on performance and emission of CI engine. *Renew. Sustain. Energy Rev.* **2013**, *27*, 664–682. [[CrossRef](#)]
11. Aransiola, E.F.; Ojumu, T.V.; Oyekola, O.; Madzimbamuto, T.; Ikhu-Omoregbe, D. A review of current technology for biodiesel production: State of the art. *Biomass Bioenergy* **2014**, *61*, 276–297. [[CrossRef](#)]
12. Li, S.; Li, X.; Ho, S.-H. Microalgae as a solution of third world energy crisis for biofuels production from wastewater toward carbon neutrality: An updated review. *Chemosphere* **2022**, *291*, 132863. [[CrossRef](#)]
13. Atabani, A.; Mahlia, T.; Masjuki, H.; Badruddin, I.A.; Yussof, H.W.; Chong, W.; Lee, K.T. A comparative evaluation of physical and chemical properties of biodiesel synthesized from edible and non-edible oils and study on the effect of biodiesel blending. *Energy* **2013**, *58*, 296–304. [[CrossRef](#)]
14. Bokhari, A.; Chuah, L.F.; Yusup, S.; Klemeš, J.J.; Akbar, M.M.; Kamil, R.N.M. Cleaner production of rubber seed oil methyl ester using a hydrodynamic cavitation: Optimisation and parametric study. *J. Clean. Prod.* **2016**, *136*, 31–41. [[CrossRef](#)]
15. Kalita, P.; Basumatary, B.; Saikia, P.; Das, B.; Basumatary, S. Biodiesel as renewable biofuel produced via enzyme-based catalyzed transesterification. *Energy Nexus* **2022**, *6*, 100087. [[CrossRef](#)]
16. Xu, H.; Li, Y.; Li, Z.; Song, Y.; Zhang, Y.; Song, H. Methane-assisted waste cooking oil conversion for renewable fuel production. *Fuel* **2022**, *311*, 122613. [[CrossRef](#)]
17. Alsaiari, M.; Ahmad, M.; Munir, M.; Zafar, M.; Sultana, S.; Dawood, S.; Almohana, A.I.; Hassan, M.H.A.-M.; Alharbi, A.F.; Ahmad, Z. Efficient application of newly synthesized green Bi₂O₃ nanoparticles for sustainable biodiesel production via membrane reactor. *Chemosphere* **2023**, *310*, 136838.
18. Huang, J.; Wang, J.; Huang, Z.; Liu, T.; Li, H. Photothermal technique-enabled ambient production of microalgae biodiesel: Mechanism and life cycle assessment. *Bioresour. Technol.* **2023**, *369*, 128390. [[CrossRef](#)]
19. Ameen, M.; Ahmad, M.; Zafar, M.; Munir, M.; Abbas, M.M.; Sultana, S.; Elkhatib, S.E.; Soudagar, M.E.M.; Kalam, M. Prospects of catalysis for process sustainability of eco-green biodiesel synthesis via transesterification: A state-of-the-art review. *Sustainability* **2022**, *14*, 7032. [[CrossRef](#)]
20. Maddikeri, G.L.; Gogate, P.R.; Pandit, A.B. Intensified synthesis of biodiesel using hydrodynamic cavitation reactors based on the interesterification of waste cooking oil. *Fuel* **2014**, *137*, 285–292. [[CrossRef](#)]

21. Jain, S.; Kumar, N.; Singh, V.P.; Mishra, S.; Sharma, N.K.; Bajaj, M.; Khan, T.Y. Transesterification of Algae Oil and Little Amount of Waste Cooking Oil Blend at Low Temperature in the Presence of NaOH. *Energies* **2023**, *16*, 1293. [[CrossRef](#)]
22. Catarino, M.; Martins, S.; Dias, A.P.S.; Pereira, M.F.C.; Gomes, J. Calcium diglyceroxide as a catalyst for biodiesel production. *J. Environ. Chem. Eng.* **2019**, *7*, 103099. [[CrossRef](#)]
23. Maleki, B.; Talesh, S.A.; Mansouri, M. Comparison of catalysts types performance in the generation of sustainable biodiesel via transesterification of various oil sources: A review study. *Mater. Today Sustain.* **2022**, *18*, 100157. [[CrossRef](#)]
24. Nawaz, S.; Ahmad, M.; Asif, S.; Klemeš, J.J.; Mubashir, M.; Munir, M.; Zafar, M.; Bokhari, A.; Mukhtar, A.; Saqib, S. Phyllosilicate derived catalysts for efficient conversion of lignocellulosic derived biomass to biodiesel: A review. *Bioresour. Technol.* **2022**, *343*, 126068. [[CrossRef](#)] [[PubMed](#)]
25. Arshad, S.; Ahmad, M.; Munir, M.; Sultana, S.; Zafar, M.; Dawood, S.; Alghamdi, A.M.; Asif, S.; Bokhari, A.; Mubashir, M. Assessing the potential of green CdO₂ nano-catalyst for the synthesis of biodiesel using non-edible seed oil of Malabar Ebony. *Fuel* **2023**, *333*, 126492. [[CrossRef](#)]
26. Ngige, G.A.; Ovuoraye, P.E.; Igwegbe, C.A.; Fetahi, E.; Okeke, J.A.; Yakubu, A.D.; Onyechi, P.C. RSM optimization and yield prediction for biodiesel produced from alkali-catalytic transesterification of pawpaw seed extract: Thermodynamics, kinetics, and Multiple Linear Regression analysis. *Digit. Chem. Eng.* **2023**, *6*, 100066. [[CrossRef](#)]
27. Kulkarni, M.G.; Dalai, A.K. Waste cooking oil an economical source for biodiesel: A review. *Ind. Eng. Chem. Res.* **2006**, *45*, 2901–2913. [[CrossRef](#)]
28. Leung, D.; Guo, Y. Transesterification of neat and used frying oil: Optimization for biodiesel production. *Fuel Process. Technol.* **2006**, *87*, 883–890. [[CrossRef](#)]
29. Orege, J.I.; Oderinde, O.; Kifle, G.A.; Ibikunle, A.A.; Raheem, S.A.; Ejeromedoghene, O.; Okeke, E.S.; Olukowi, O.M.; Orege, O.B.; Fagbohun, E.O. Recent advances in heterogeneous catalysis for green biodiesel production by transesterification. *Energy Convers. Manag.* **2022**, *258*, 115406. [[CrossRef](#)]
30. Mardiana, S.; Azhari, N.J.; Ilmi, T.; Kadja, G.T. Hierarchical zeolite for biomass conversion to biofuel: A review. *Fuel* **2022**, *309*, 122119. [[CrossRef](#)]
31. Tan, X.; Zhang, H.; Li, H.; Yang, S. Electrovalent bifunctional acid enables heterogeneously catalytic production of biodiesel by (trans) esterification of non-edible oils. *Fuel* **2022**, *310*, 122273. [[CrossRef](#)]
32. Nabgan, W.; Nabgan, B.; Ikram, M.; Jadhav, A.H.; Ali, M.W.; Ul-Hamid, A.; Nam, H.; Lakshminarayana, P.; Bahari, M.B.; Khusunun, N.F. Synthesis and catalytic properties of calcium oxide obtained from organic ash over a titanium nanocatalyst for biodiesel production from dairy scum. *Chemosphere* **2022**, *290*, 133296. [[CrossRef](#)]
33. Okechukwu, O.D.; Joseph, E.; Nonso, U.C.; Kenechi, N.-O. Improving heterogeneous catalysis for biodiesel production process. *Clean. Chem. Eng.* **2022**, *3*, 100038. [[CrossRef](#)]
34. Sharma, T.; Velmurugan, N.; Patel, P.; Chon, B.; Sangwai, J. Use of oil-in-water pickering emulsion stabilized by nanoparticles in combination with polymer flood for enhanced oil recovery. *Pet. Sci. Technol.* **2015**, *33*, 1595–1604. [[CrossRef](#)]
35. Santos, S.; Puna, J.; Gomes, J. A Brief Review of the Supercritical Antisolvent (SAS) Technique for the Preparation of Nanocatalysts to Be Used in Biodiesel Production. *Energies* **2022**, *15*, 9355. [[CrossRef](#)]
36. Zhang, Y.; Duan, L.; Esmaeili, H. A review on biodiesel production using various heterogeneous nanocatalysts: Operation mechanisms and performances. *Biomass Bioenergy* **2022**, *158*, 106356. [[CrossRef](#)]
37. Topare, N.S.; Gujarathi, V.S.; Bhattacharya, A.A.; Bhoyar, V.M.; Shastri, T.J.; Manewal, S.P.; Gomkar, C.S.; Khedkar, S.V.; Khan, A.; Asiri, A.M. A review on application of nano-catalysts for production of biodiesel using different feedstocks. *Mater. Today: Proc.* **2023**, *72*, 324–335. [[CrossRef](#)]
38. Ahmad, M.; Elnaggar, A.Y.; Teong, L.K.; Sultana, S.; Zafar, M.; Munir, M.; Hussein, E.E.; Abidin, S.Z.U. Sustainable and eco-friendly synthesis of biodiesel from novel and non-edible seed oil of *Monothecha buxifolia* using green nano-catalyst of calcium oxide. *Energy Convers. Manag. X* **2022**, *13*, 100142.
39. Vignesh, P.; Jayaseelan, V.; Pugazhendiran, P.; Prakash, M.S.; Sudhakar, K. Nature-inspired nano-additives for Biofuel application—A Review. *Chem. Eng. J. Adv.* **2022**, *12*, 100360. [[CrossRef](#)]
40. Jabeen, M.; Munir, M.; Abbas, M.M.; Ahmad, M.; Waseem, A.; Saeed, M.; Kalam, M.A.; Zafar, M.; Sultana, S.; Mohamed, A. Sustainable production of biodiesel from novel and non-edible *Ailanthus altissima* (Mill.) seed oil from green and recyclable potassium hydroxide activated *Ailanthus* cake and cadmium sulfide catalyst. *Sustainability* **2022**, *14*, 10962. [[CrossRef](#)]
41. Foidl, N.; Foidl, G.; Sanchez, M.; Mittelbach, M.; Hackel, S. *Jatropha curcas* L. as a source for the production of biofuel in Nicaragua. *Bioresour. Technol.* **1996**, *58*, 77–82. [[CrossRef](#)]
42. Choe, E.; Min, D.B. Mechanisms and factors for edible oil oxidation. *Compr. Rev. Food Sci. Food Saf.* **2006**, *5*, 169–186. [[CrossRef](#)]
43. Ullah, K.; Jan, H.A.; Ahmad, M.; Ullah, A. Synthesis and structural characterization of biofuel from *Cocklebur* sp., using zinc oxide nano-particle: A novel energy crop for bioenergy industry. *Front. Bioeng. Biotechnol.* **2020**, *8*, 756. [[CrossRef](#)] [[PubMed](#)]
44. Ahmad, M.; Rajapaksha, A.U.; Lim, J.E.; Zhang, M.; Bolan, N.; Mohan, D.; Vithanage, M.; Lee, S.S.; Ok, Y.S. Biochar as a sorbent for contaminant management in soil and water: A review. *Chemosphere* **2014**, *99*, 19–33. [[CrossRef](#)] [[PubMed](#)]
45. Nagarajan, P.; Gurunathan, B.; Pandian, S.; Karuppasamy, I.; Ramakrishnan, G.; Sahadevan, R. Efficient utilization of seed biomass and its by-product for the biodiesel production. In *Biofuels and Bioenergy*; Elsevier: Amsterdam, The Netherlands, 2022; pp. 483–493.

46. Ameen, M.; Zafar, M.; Ramadan, M.F.; Ahmad, M.; Makhkamov, T.; Bokhari, A.; Mubashir, M.; Chuah, L.F.; Show, P.L. Conversion of novel non-edible *Bischofia javanica* seed oil into methyl ester via recyclable zirconia-based phyto-nanocatalyst: A circular bioeconomy approach for eco-sustenance. *Environ. Technol. Innov.* **2023**, *30*, 103101. [[CrossRef](#)]
47. Asemani, M.; Anarjan, N. Green synthesis of copper oxide nanoparticles using *Juglans regia* leaf extract and assessment of their physico-chemical and biological properties. *Green Process. Synth.* **2019**, *8*, 557–567. [[CrossRef](#)]
48. Suresh, T.; Sivarajasekar, N.; Balasubramani, K. Enhanced ultrasonic assisted biodiesel production from meat industry waste (pig tallow) using green copper oxide nanocatalyst: Comparison of response surface and neural network modelling. *Renew. Energy* **2021**, *164*, 897–907. [[CrossRef](#)]
49. Narasaiah, P.; Mandal, B.K.; Sarada, N. Biosynthesis of copper oxide nanoparticles from *Drypetes sepiaria* leaf extract and their catalytic activity to dye degradation. *Proc. IOP Conf. Ser. Mater. Sci. Eng.* **2017**, *263*, 022012. [[CrossRef](#)]
50. Raul, P.K.; Senapati, S.; Sahoo, A.K.; Umlong, I.M.; Devi, R.R.; Thakur, A.J.; Veer, V. CuO nanorods: A potential and efficient adsorbent in water purification. *Rsc Adv.* **2014**, *4*, 40580–40587. [[CrossRef](#)]
51. Yedurkar, S.; Maurya, C.; Mahanwar, P. Biosynthesis of zinc oxide nanoparticles using *ixora coccinea* leaf extract—A green approach. *Open J. Synth. Theory Appl.* **2016**, *5*, 1–14. [[CrossRef](#)]
52. Mahamuni, N.N.; Adewuyi, Y.G. Fourier transform infrared spectroscopy (FTIR) method to monitor soy biodiesel and soybean oil in transesterification reactions, petrodiesel–biodiesel blends, and blend adulteration with soy oil. *Energy Fuels* **2009**, *23*, 3773–3782. [[CrossRef](#)]
53. Chakrabarti, M.; Ali, M.; Baroutian, S.; Saleem, M. Techno-economic comparison between B10 of *Eruca sativa* L. and other indigenous seed oils in Pakistan. *Process Saf. Environ. Prot.* **2011**, *89*, 165–171. [[CrossRef](#)]
54. Qavami, N.; Naghdi, B.H.; Labbafi, M.; Mehrafarin, A. A review on pharmacological, cultivation and biotechnology aspects of milk thistle (*Silybum marianum* (L.) Gaertn.). *J. Med. Plants* **2013**, *12*, 19–37.
55. Dhar, A.; Kevin, R.; Agarwal, A.K. Production of biodiesel from high-FFA neem oil and its performance, emission and combustion characterization in a single cylinder DIC engine. *Fuel Process. Technol.* **2012**, *97*, 118–129. [[CrossRef](#)]
56. Naik, M.; Meher, L.; Naik, S.; Das, L. Production of biodiesel from high free fatty acid Karanja (*Pongamia pinnata*) oil. *Biomass Bioenergy* **2008**, *32*, 354–357. [[CrossRef](#)]
57. Sarve, A.; Sonawane, S.S.; Varma, M.N. Ultrasound assisted biodiesel production from sesame (*Sesamum indicum* L.) oil using barium hydroxide as a heterogeneous catalyst: Comparative assessment of prediction abilities between response surface methodology (RSM) and artificial neural network (ANN). *Ultrason. Sonochem.* **2015**, *26*, 218–228. [[CrossRef](#)]
58. Al-Hamamre, Z.; Al-Mater, A.; Sweis, F.; Rawajfeh, K. Assessment of the status and outlook of biomass energy in Jordan. *Energy Convers. Manag.* **2014**, *77*, 183–192. [[CrossRef](#)]
59. Hasni, K.; Ilham, Z.; Dharma, S.; Varman, M. Optimization of biodiesel production from *Brucea javanica* seeds oil as novel non-edible feedstock using response surface methodology. *Energy Convers. Manag.* **2017**, *149*, 392–400. [[CrossRef](#)]

Disclaimer/Publisher’s Note: The statements, opinions and data contained in all publications are solely those of the individual author(s) and contributor(s) and not of MDPI and/or the editor(s). MDPI and/or the editor(s) disclaim responsibility for any injury to people or property resulting from any ideas, methods, instructions or products referred to in the content.